Fate of Thermalization of Ultracold Fermions with Two-Body Dissipation

Xin-Yuan Gao[1] and Yangqian Yan[1,2,*]
[1]Department of Physics, The Chinese University of Hong Kong, Shatin, New Territories, Hong Kong, China
[2]The Chinese University of Hong Kong Shenzhen Research Institute, 518057 Shenzhen, China

(Received 23 October 2024; accepted 25 March 2025; published 17 April 2025)

Two-body inelastic collisions arising from chemical reactions are prevalent in ultracold fermionic and bosonic molecular gases. Although recent advancements have achieved quantum degeneracy in these systems, loss dynamics are typically modeled phenomenologically using rate equations that often assume thermalization during chemical reactions. In this study, we employ the inelastic quantum Boltzmann equation to analyze particle loss, temperature evolution, and momentum distributions in single-component Fermi gases from first principles. Our results demonstrate that the conventional particle-number rate equation accurately describes the dynamics in trapped systems but fails to capture the behavior in homogeneous systems. Notably, under pure p-wave inelastic collisions and zero elastic collisions, we find that systems prepared near or above quantum degeneracy remain in a thermal state, whereas systems initialized deep within degeneracy exhibit nonequilibrium dynamics. Our theoretical predictions align well with recent experimental observations in trapped systems, and our claim can be further verified in atomic systems with induced two-body loss in box potentials.

DOI: 10.1103/PhysRevLett.134.153402

Introduction—In classical hydrodynamic theory, dissipation, which originates from the inelastic collisions between particles and leads to heating, has been extensively studied in granular fluids [1–5]. Correspondingly, similar dissipative phenomena have also been observed in the quantum regime. A vital feature of ultracold molecular gases—one of the candidates for quantum simulation [6–13] and quantum computation [14–17]—is their two-body losses due to either chemical reactions or light-assisted chemical reaction, which are intrinsic to both fermions [18–23] and bosons [24–29].

After the preparation of the dissipative ultracold molecular systems, it has been observed that the system can be fitted with thermal profiles, with a gradually increasing temperature. This process has been dubbed antievaporation [30,31]. While the system appears thermal and the temperature dynamics can be modeled using phenomenological rate equations [26,27,32–36], it is not yet fully clear whether the system stays in a genuine thermal state under a long-time dissipation. For single-component bosonic systems with inelastic s-wave interactions, where the potential has no momentum dependence in Fourier space, particles with different momenta are removed at the same rate, leaving the shape of momentum distribution unchanged. Conversely, for single-component fermionic systems with inelastic p-wave interactions, the intrinsic momentum dependence of the interaction leads to particles with different momenta being removed at different rates. Thus, two-body p-wave loss could push the system out of thermal equilibrium and lead to exotic physics.

We now focus on single-component fermions with p-wave interactions. Although local thermal equilibrium could be assumed for classicial fluids, this may not be the case for ultracold molecules. It has been verified that a molecular gas could be thermalized with atom-molecule collision [37], and theories assuming a thermalized density matrix remain valid in a short time window [38–41]. However, thermal equilibrium may not last a long time for a pure fermionic molecular quantum gas because the relaxation time (e.g., several minutes [42]) could be much longer than the characteristic two-body decay time (seconds). This seemingly forbids thermal equilibrium in long-term dynamics. There have been numerical studies of long-term dynamics using Lindblad equations [43,44], yet agreement with experiments has not been achieved under typical experimental parameters.

This Letter attempts to address the fate of thermalization for single-component Fermi gases with two-body p-wave inelastic loss at finite temperatures by analyzing the *long-time dynamics* from first principles. (i) We solve the inelastic quantum Boltzmann equation in the zero and infinitely fast elastic collision limit for systems in harmonic and box potentials. (ii) For harmonically trapped systems, our theory reproduces the long-time dynamics in experiments without any fitting parameter. We find that the solution almost agrees with the conventional two-body particle-number decay equation for harmonically trapped systems at high initial temperatures. (iii) In box traps, we obtain analytical (numerical) decay dynamics for arbitrary

*Contact author: yqyan@cuhk.edu.hk

initial temperatures in the zero (strong) elastic collision limit and predict an unconventional particle-number decay equation that could be tested in ultracold atomic experiments.

Model—To describe a weakly interacting and reactive single-component Fermi gas, we begin with the single-channel p-wave non-Hermitian interaction:

$$\hat{U} = \frac{3g}{2V} \sum_{\mathbf{P},\mathbf{q},\mathbf{q}'} \mathbf{q}\cdot\mathbf{q}' c^\dagger_{\frac{\mathbf{P}}{2}+\mathbf{q}} c^\dagger_{\frac{\mathbf{P}}{2}-\mathbf{q}} c_{\frac{\mathbf{P}}{2}-\mathbf{q}'} c_{\frac{\mathbf{P}}{2}+\mathbf{q}'}, \tag{1}$$

with coupling strength $g = 4\pi\hbar^2[\mathrm{Re}(v_p) + i\,\mathrm{Im}(v_p)]/M$ derived from the low-energy p-wave phase shift: $k^3\cot(\delta_p) = -1/v_p + \mathcal{O}(k^2)$. Here, we neglected higher order contributions such as the effective range as its contribution to loss is small in typical experimental conditions [41]. The model is a direct generalization of s-wave complex contact interaction [45]. Here, v_p, M, and V are the complex p-wave scattering volume v_p, the particle mass, and the system's volume, respectively, and $c_\mathbf{k}$ is the fermionic annihilation operator following the canonical anticommutation relation. By expanding the dynamics of $\langle N_\mathbf{k}\rangle = \langle c^\dagger_\mathbf{k} c_\mathbf{k}\rangle$ up to the second order of the interaction [42], we obtain the inelastic Boltzmann equation that governs the dynamics of a homogeneous system:

$$dn_\mathbf{k}/dt = \mathcal{I}_\mathrm{inel}[n_\mathbf{k}V]/V + \mathcal{I}_\mathrm{el}[n_\mathbf{k}V]/V, \tag{2}$$

where $n_\mathbf{k}(t) = \langle N_\mathbf{k}\rangle(t)/V$ is the momentum distribution function and $\mathcal{I}_\mathrm{inel}[n_\mathbf{k}V]$ and $\mathcal{I}_\mathrm{el}[n_\mathbf{k}V]$ are the inelastic and elastic collision integrals, respectively. Specifically, the inelastic collision integral is given by

$$\mathcal{I}_\mathrm{inel}[n_\mathbf{k}V] = \frac{12\pi\hbar\,\mathrm{Im}(v_p)V^2}{M}\int \frac{d^3q}{(2\pi)^3}(q^2+k^2)n_\mathbf{k}n_\mathbf{q}, \tag{3}$$

and the form of the elastic collision integral $\mathcal{I}_\mathrm{el}[n_\mathbf{k}]$ can be found in the companion paper [42]. For application to typical molecular Fermi gas in experiments, $\mathcal{I}_\mathrm{el}$ can be safely ignored because the relaxation time is much longer than other time scales in the system [42]. Equation (3) has also been derived by Ref. [44] using a two-channel model. Similar forms of inelastic collision integrals can also be obtained in strongly interacting Bose gases with two-body losses in 1D [46–48].

To accurately model ultracold gas experiments, which are predominantly conducted in harmonic traps, we adapt Eq. (2) using the local-density approximation $n_\mathbf{k}V \to f(\mathbf{k},\mathbf{r})$, where $f(\mathbf{k},\mathbf{r})$ represents the phase space density. In addition to elastic and inelastic collisions, the inhomogeneity prompts the cloud to flow. The inelastic Boltzmann equation in harmonic traps governing the complete set of dynamics is thus

$$\frac{df}{dt} = \left[-\frac{\hbar\mathbf{k}\cdot\nabla_\mathbf{r}}{M} + \frac{\nabla_\mathbf{r}U_\mathrm{ext}\cdot\nabla_\mathbf{k}}{\hbar}\right]f + \mathcal{I}_\mathrm{inel}[f] + \mathcal{I}_\mathrm{el}[f], \tag{4}$$

where $U_\mathrm{ext}(\mathbf{r}) = \sum_{i=x,y,z} M\omega_i^2 r_i^2/2$ is the external harmonic trapping potential, with ω_i denoting the trapping angular frequencies in the three spatial directions.

We analyze two limiting scenarios: (i) zero elastic collisions, where dynamics are governed purely by inelastic processes, and (ii) infinitely fast elastic collisions (thermal ansatz), where momentum redistribution is instantaneous, maintaining thermal equilibrium. For typical experiments where elastic relaxation times far exceed loss times [42], scenario (i) better describes reality, while comparing with scenario (ii) helps quantify deviations from thermalization. Under thermal ansatz, the dynamics reduce to coupled equations for particle number and temperature, detailed in [42].

Conventionally, for a two-body loss, denoting the total number of particles to be $N(t) = \int d^3k n_\mathbf{k}(t)/(2\pi)^3$ or $\int d^3r d^3k f(\mathbf{r},\mathbf{k},t)/(2\pi)^3$, it is most natural to expect the dynamics to be [49]

$$dN(t)/dt \propto -N(t)^\mathcal{N}, \tag{5}$$

where $\mathcal{N} = 2$. Though this holds for s-wave interactions, we will demonstrate later that in single-component Fermi gases with collisions of p-wave nature, the two-body loss dynamics may lead to $\mathcal{N} \neq 2$.

Harmonically trapped systems—We first consider systems loaded into a harmonic trap, where the dynamics are described by Eq. (4). As a general feature of the Boltzmann equation, Eq. (4) has an irreducible six-dimensional spatial complexity, making it hard to solve. Nevertheless, there exists a separation of time scales, which simplifies the problem. The harmonic trap tends to average the phase space distribution $f(\mathbf{r},\mathbf{k},t)$ such that it has a spherical symmetry in the whole phase space, i.e., defining $R(t) = \sqrt{\sum_{i=x,y,z}\{[k_i/k_F^\mathrm{trap}(t)]^2 + [\omega_i r_i/\omega r_F(t)]^2\}}$, $f(\mathbf{r},\mathbf{k},t) \equiv f(R,t)$, where $k_F^\mathrm{trap}(t) = [48N(t)]^{1/6}\sqrt{M\omega/\hbar}$ and $r_F(t) = [48N(t)]^{1/6}\sqrt{\hbar/M\omega}$ are the Fermi momentum and Thomas-Fermi radius of the harmonically trapped system, respectively, with $\omega = (\omega_x\omega_y\omega_z)^{1/3}$ being the geometric mean of angular frequencies of the harmonic trap. Indeed, this is the steady-state solution without the inelastic term. Despite the fact that the inelastic collisions drive the phase space density into asymmetric forms, under typical experimental parameters, two-body dissipation has a much longer time scale (usually on the order of s) compared to that of cloud-flowing determined by trap frequencies (typically on the order of ms). Thus, we propose a fast-flowing approximation, which assumes that the phase space distribution is always in the spherical form. This could be understood as the following: though the inelastic collision tries to bring asymmetry to the

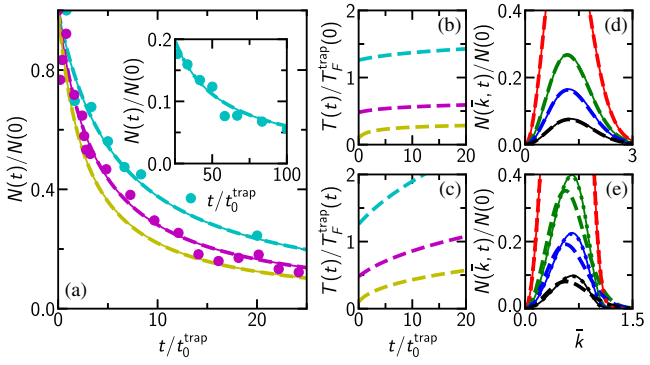

FIG. 1. Long-time dynamics of the trapped single-component Fermi gases with inelastic p-wave interactions. (a) Total number of particles as a function of time. Symbols, solid lines, and dashed lines are experimental data from Ref. [50], numerical results solved from the inelastic Boltzmann equation [Eq. (4)] under the fast-flow approximation, and results obtained from thermal ansatz, respectively. From top to bottom, cyan, magenta, and yellow denote initial temperatures $T = 1.26$, 0.48, and $0.1T_F^{\rm trap}(0)$, respectively [for experimental data, we set $N(0) = 46000$ and 8400 at high and medium temperatures, respectively]. Inset: longer time dynamics for $T(0)/T_F^{\rm trap}(0) = 1.26$. (b),(c) Dynamics of physical and reduced temperatures of thermal ansatz. Colors have the same meaning as those in (a). (d),(e) Evolution of radial momentum distribution for $T(0)/T_F^{\rm trap}(0) = 1.26$ and 0.1, respectively. From top to bottom at $\bar{k} = 0.7$, red, green, blue, and black denote $t/t_0^{\rm trap} = 0$, 10, 20, 50, respectively. Solid lines and dotted lines represent numerical results under fast-flow approximation and its quasithermal profile fit, respectively; the dashed line is for the thermal ansatz.

distribution, the trap term restores the symmetry at a much faster rate. We have validated this approximation through a quasi-1D analogy of Eq. (4) in the companion paper [42]. It is noted that the fast-flowing approximation is closely related to the basic assumption of Chapman-Enskog expansion in classic hydrodynamics, where the collision, rather than flowing, is assumed to have the fastest timescale enforcing system obeying the steady state of the collision integral.

Under the fast-flowing approximation, we numerically solve Eq. (4) and demonstrate results starting with systems above, near, and in the deep degeneracy ($T(0)/T_F^{\rm trap} = 1.26$, 0.48, and 0.1, respectively) in Fig. 1(a). For convenience, we set the unit $t_0^{\rm trap} = 4M/(\pi\hbar[k_F^{\rm trap}(0)]^5|\,{\rm Im}(v_p)|)$. We have compared our calculation with experimental data provided in Ref. [50] for the first two cases and shown that they agree well for long times (both situations correspond to approximately 6 seconds in the experiment [20]). We note that the short-time limit of the number dynamics agrees with the contact-loss relation explored in previous works [39,41] and is also consistent with the temperature-dependent loss rate measurements [42].

To investigate the system's thermalization during evolution, we also solve the inelastic quantum Boltzmann equation under thermal ansatz and compare the result with our numerical results. The fast-flowing approximation is exact for systems in the equilibrium limit since the thermal ansatz naturally respects spherical symmetry in the phase space. We assume that initially, the system starts from an equilibrated state at a temperature T. The thermal ansatz then means that $f^{\rm th}(\mathbf{k},\mathbf{r})(t)$ always has the shape of a Fermi-Dirac distribution, but with varying temperature $T(t)$ and Fermi temperature $T_F^{\rm trap}(t) = \hbar^2[k_F^{\rm trap}(t)]^2/2Mk_B$, i.e., $f^{\rm th}(\mathbf{k},\mathbf{r}) \equiv f^{\rm th}[R(t),t] = \{\exp[R(t)^2/[T(t)/T_F^{\rm trap}(t)]]\,(z^{\rm th,trap})^{-1} + 1\}^{-1}$, where $z^{\rm th,trap} = -{\rm Li}_3(-z^{\rm th,trap}) = [T(t)/T_F^{\rm trap}(t)]^{-3}/6$ with ${\rm Li}_s$ denoting the polylogarithm function. Figure 1(a) shows that the thermal ansatz closely matches the fast-flowing approximation predictions for particle-number dynamics. This observation provides insight into why a phenomenological two-body decay equation describes the system well in this case: in the high-initial-temperature limit $T(0)/T_F^{\rm trap}(0) \to \infty$, we derive an analytical solution based on the thermal ansatz [42]:

$$N(t) = N(0)/[1 + C(t/t_0^{\rm trap})]^{0.960}, \tag{6}$$

where $C = 0.198418/\sqrt{T(0)/T_F^{\rm trap}(0)}$. Applying Eq. (5) to Eq. (6) yields $\mathcal{N} = 2.04167$, which is nearly the conventional two-body behavior ($\mathcal{N} \approx 2$). This behavior is independent of the trap frequencies as long as they are larger than the characteristic two-body loss frequency.

Through the temperature dynamics of thermal ansatz, we can also reproduce the antievaporation without introducing an artificial heating term [44]. Below, we present the results in two complementary ways. First, Fig. 1(b) illustrates the dynamics of the "physical temperature," using $T_F^{\rm trap}(0)$ as a fixed unit to characterize the average particle energy. Second, Fig. 1(c) displays the "reduced temperature," where $T_F^{\rm trap}(t)$ evolves with the total particle number, indicating whether the system is in a "high-temperature" or "low-temperature" regime. Analysis of both physical and reduced temperature evolution [Figs. 1(b) and 1(c)] shows that both temperatures increase regardless of initial conditions, which is consistent with the antievaporation phenomena observed in experiments, i.e., density-dependent loss leads to faster depletion at trap center, causing cloud expansion and effective heating that dominates the dynamics.

Finally, we examine the momentum distribution evolution $[N(\bar{k},t) = 4\pi\bar{k}^2\int d^3r f(\mathbf{r},\mathbf{k},t)/(2\pi)^3$, where $\bar{k} = k/k_F^{\rm trap}(0)]$. Systems starting above degeneracy are well described by the corresponding thermal ansatz [Fig. 1(d)], while those beginning in deep degeneracy exhibit nonequilibrium behavior [Fig. 1(e)]. It is worthwhile to note that, though thermal ansatz does not agree well with the low-temperature evolution, a "quasithermal profile," i.e., fit time-of-flight images to a general

Fermi-Dirac distribution with three parameters of prefactor, T, and fugacity z, can still be made and agrees with the momentum distribution well. In fact, this could be a typical practice in experiments as the prefactor originates from absorption imaging. Figures 1(d) and 1(e) demonstrate that this quasithermal profile fits the fast-flowing approximation results well, even for low initial temperatures and long-time evolution. Consequently, experimental measurements may conclude that the system is "thermalized" based on this criterion.

Box potential—Though our theory explains existing experiments without fitting parameters, they could still be approximated well by thermal ansatz or even a naive rate equation. This "disappointing" result comes from the trap averaging: the harmonic trap provides a force in the momentum space such that it induces a flow in phase space seemingly towards a thermal state. Fortunately, nowadays, experiments are also performed in box traps [51], where this unwanted flow does not exist. In this case, the problem is even simpler as we only need to evolve the three-dimensional momentum distribution instead of the six-dimensional phase space distribution.

Again, we assume that the system starts from an equilibrated state at temperature T. Thus, $n_{\mathbf{k}}(0)$ simply follows the Fermi-Dirac distribution $n_{\mathbf{k}}(0) = [\exp(\hbar^2 k^2/2Mk_BT)z(T)^{-1} + 1]^{-1}$. The fugacity $z(T)$ is implicitly determined by $-\mathrm{Li}_{3/2}[-z(T)] = 4\bar{T}^{-3/2}/3\sqrt{\pi}$, where $\bar{T} = T/T_F(0)$ and $T_F(0) = \hbar^2[6\pi^2 N(0)/V]^{2/3}/2M$. Utilizing Mellin transformation, in the zero elastic collision limit, we find an accurate approximation of $N(t)$ [42]

$$N(t) = N(0)[1 + (F_1 + F_2/F_1)(t/t_0)]^{\frac{-2F_1^2}{F_1^2+F_2}}, \tag{7}$$

where $F_j = -\frac{3}{2}\bar{T}^{\frac{3}{2}+j}\Gamma(3/2+j)\mathrm{Li}_{\frac{3}{2}+j}[-z(T)]$ and $t_0 = M/(12\pi\hbar k_F^5(0)|\mathrm{Im}(v_p)|)$ is the time unit; the homogeneous Fermi momentum is $k_F(t) = [6\pi^2 N(t)/V]^{1/3}$.

Solid lines and symbols in Fig. 2(a) demonstrate the comparison between Eq. (7) and brute-force numerical solution, showing that the approximation is satisfactory within a reasonably long time window. It is noted that Eq. (7) is the solution of Eq. (5) with

$$\mathcal{N} = 3/2 + F_2/(2F_1^2); \tag{8}$$

thus, one may regard the dissipation dynamics as an $\mathcal{N}$-body process in the conventional sense. The inset of Fig. 2(a) shows $\mathcal{N}$ against $\bar{T}$, where we observe that $\mathcal{N}$ monotonically decreases with $\bar{T}$. It is straightforward to obtain the limits $\mathcal{N}(\bar{T}\to 0) = 44/21$ and $\mathcal{N}(\bar{T}\to\infty) = 7/3$. Note that Eq. (7) is exact in the limit $\bar{T}\to\infty$, where the full dynamics of $n_{\mathbf{k}}(t)$ is [42]

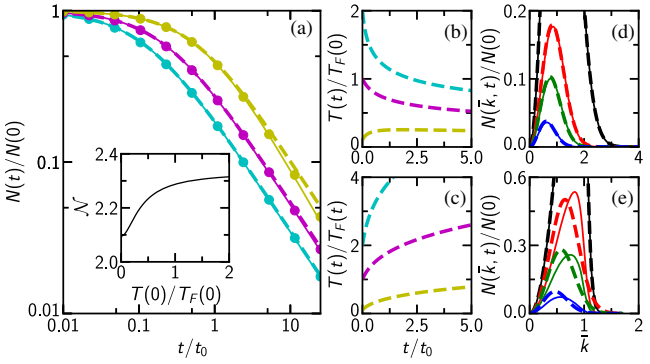

FIG. 2. Long-time dynamics of single-component Fermi gases with inelastic p-wave collisions in box potential. (a) Total number of particles as a function of time t. Circles, solid lines, and dashed lines represent the numerical solution of the inelastic Boltzmann equation [Eq. (2) ignoring elastic collision integral], the analytical approximation [Eq. (7)], and the solution based on thermal ansatz, respectively. From top to bottom, yellow, magenta, and cyan denote the initial temperatures $T(0) = 0.1$, 1, and $2T_F(0)$, respectively. Inset: the N-body indicator [Eq. (8)] as a function of the initial temperature $T(0)$. (b),(c) the physical temperature in units of $T_F(0)$ and the reduced temperature as a function of time, respectively; from top to bottom, the yellow, magenta, and cyan lines correspond to initial temperatures $T(0) = 0.1$, 1, and $2T_F(0)$, respectively. (d),(e) the dynamics of the radial momentum distribution of the system with initial temperature $T(0) = 2T_F(0)$ and $T(0) = 0.1T_F(0)$, respectively. Solid and dashed lines denote brute-force numerical solution of the inelastic Boltzmann equation and results based on thermal ansatz, respectively. Black, red, green, and blue denote $t/t_0 = 0$, 2, 5, 25, respectively.

$$n_{\mathbf{k}}(t) = \frac{4\exp[-\bar{k}^2(1+4\bar{T}t)^{\frac{1}{4}}/\bar{T}t_0]}{3\sqrt{\pi}N(0)\bar{T}^{\frac{3}{2}}(1+4\bar{T}t/t_0)^{\frac{8}{3}}}, \tag{9}$$

where $\bar{k} = k/k_F(0)$.

To rigorously check whether the system thermalizes after a long time evolution, we solve Eq. (2) under the thermal ansatz with varying $T(t)$ and $T_F(t) = \hbar^2[k_F(t)]^2/2Mk_B$, i.e., $n_{\mathbf{k}}^{\mathrm{th}}(t) = \{\exp[[k/k_F(t)]^2/[T(t)/T_F(t)]]z^{\mathrm{th}}(t)^{-1} + 1\}^{-1}$, where $-\mathrm{Li}_{3/2}[-z^{\mathrm{th}}(t)] = 4[T(t)/T_F(t)]^{-3/2}/3\sqrt{\pi}$. In the high-initial-temperature limit $T(0)/T_F(0)\to\infty$, there are simple solutions [42]: $N(t) = N(0)/[1+4\bar{T}(0)t/t_0]^{\frac{3}{4}}$ and $T(t) = T(0)/[1+4\bar{T}(0)t/t_0]^{\frac{1}{4}}$. Substituting back to the thermal ansatz and taking the high-temperature limit, one recovers Eq. (9), confirming that the system continually evolves under thermalized profiles even strictly without elastic collisions. Note that the high-temperature long-time power-law decay has also been reported in arbitrary dimensions [52].

To determine whether systems at finite temperatures thermalize, we numerically evaluate the thermal ansatz to calculate $N(t)/N(0)$ and compare it with Eq. (7). Similar to harmonically trapped systems, we plot the results in terms

of "physical temperatures" [Fig. 2(b)] and "reduced temperatures" [Fig. 2(c)]. The physical temperature dynamics strongly depend on the initial temperature. (i) It decreases for systems initially above or near quantum degeneracy. This is because high-momentum particles are more likely to tunnel through the p-wave barrier and undergo collisions, as reflected in the momentum dependence of Eq. (3). Consequently, p-wave collisions preferentially remove higher-energy particles, reducing the average energy and, thus, the physical temperature. (ii) In the deeply degenerate regime, any perturbation to the Fermi sea structure, including dissipation, tends to heat the system, thus increasing the physical temperature. In contrast, reduced temperatures always increase, indicating that p-wave inelastic collisions invariably drive the system away from quantum degeneracy and ultimately into the high-temperature regime. Note that, in comparison, harmonically trapped systems [Figs. 1(b) and 1(c)] behave rather differently due to the extra dynamics of the shape.

Interestingly, in homogeneous systems, particularly those starting from low initial temperatures, the quasithermal profile fails to provide an excellent fit. Instead, we find that the long-time asymptote of the radial momentum distribution in homogeneous systems follows $N(\bar{k}, t \to \infty) \propto \exp(-\alpha\bar{k}^2)\bar{k}^{19/2}$ in the zero initial temperature limit (see our companion paper [42]), where α is a constant. In contrast, the quasithermal profile can only fit $\exp(-\alpha\bar{k}^2)\bar{k}^2$, further highlighting the distinct behavior between homogeneous and harmonically trapped systems.

Returning to particle-number dynamics, dashed lines in Fig. 2(a) show the thermal-ansatz predictions. For systems near or above quantum degeneracy ($\bar{T} = 1$ and 2), $\mathcal{N}$ is approximately the same value at the high-temperature limit $7/3$, and we also observe that the solution from Eq. (7) agrees well with the thermal ansatz. However, in deeply degenerate systems ($\bar{T} = 0.1$), $\mathcal{N}$ is approximately 2.1, and a notable discrepancy in the number of particles emerges in the long-time tail. Correspondingly, we present the evolution of the radial momentum distribution $N(\bar{k}) = 4\pi\bar{k}^2 n_{\mathbf{k}} V/(2\pi)^3$ in Figs. 2(d) and 2(e) for these two distinct cases: $\bar{T} = 1$ and $\bar{T} = 0.1$. At $\bar{T} = 1$, the two are virtually indistinguishable, underscoring the close approximation to thermalization in near-degenerate conditions. Conversely, a discernible difference emerges between the two profiles at the deeply degenerate temperature $\bar{T} = 0.1$.

Conclusion—To summarize, we derived the inelastic quantum Boltzmann equation for single-component fermi gases with two-body loss and theoretically studied the long-time thermalization dynamics. Our first-principle calculations explain experiments in traps without fitting parameters and provide physical insights into the "anti-evaporation" phenomena. Our prediction that the low-temperature lossy system becomes nonthermal could be further verified using atoms such as Li and K loaded in optical boxes, where the two-body loss could be induced using optical Feshbach resonance or dipolar relaxation [53–62]. Our particle-number loss curve could serve as a thermometer for box-trapped systems. In addition, our work serves as valuable benchmarks for calibrating relevant Direct Simulation Monte Carlo simulations [63] and contact measurements using two-body loss in p-wave BCS-BEC crossover studies in the future.

Acknowledgments—We would like to acknowledge financial support from the National Natural Science Foundation of China under Grant No. 124B2074 and No. 12204395, Hong Kong RGC Early Career Scheme under Grant No. 24308323 and Collaborative Research Fund under Grant No. C4050-23GF, the Space Application System of China Manned Space Program, and CUHK under Direct Grant No. 4053676. We thank Zhigang Wu, Doerte Blume, and Kaiyuen Lee for their helpful discussions.

[1] N. Sela and I. Goldhirsch, Hydrodynamic equations for rapid flows of smooth inelastic spheres, to Burnett order, J. Fluid Mech. **361**, 41 (1998).
[2] V. Garzó and J. W. Dufty, Dense fluid transport for inelastic hard spheres, Phys. Rev. E **59**, 5895 (1999).
[3] E. Ben-Naim, S. Y. Chen, G. D. Doolen, and S. Redner, Shocklike dynamics of inelastic gases, Phys. Rev. Lett. **83**, 4069 (1999).
[4] A. V. Bobylev, J. A. Carrillo, and I. M. Gamba, On some properties of kinetic and hydrodynamic equations for inelastic interactions, J. Stat. Phys. **98**, 743 (2000).
[5] E. Ben-Naim and P. L. Krapivsky, Scaling, multiscaling, and nontrivial exponents in inelastic collision processes, Phys. Rev. E **66**, 011309 (2002).
[6] A. Micheli, G. K. Brennen, and P. Zoller, A toolbox for lattice-spin models with polar molecules, Nat. Phys. **2**, 341 (2006).
[7] L. D. Carr, D. DeMille, R. V. Krems, and J. Ye, Cold and ultracold molecules: Science, technology and applications, New J. Phys. **11**, 055049 (2009).
[8] K. Osterloh, N. Barberán, and M. Lewenstein, Strongly correlated states of ultracold rotating dipolar Fermi gases, Phys. Rev. Lett. **99**, 160403 (2007).
[9] H. P. Büchler, E. Demler, M. Lukin, A. Micheli, N. Prokof'ev, G. Pupillo, and P. Zoller, Strongly correlated 2D quantum phases with cold polar molecules: Controlling the shape of the interaction potential, Phys. Rev. Lett. **98**, 060404 (2007).
[10] A. V. Gorshkov, S. R. Manmana, G. Chen, J. Ye, E. Demler, M. D. Lukin, and A. M. Rey, Tunable superfluidity and quantum magnetism with ultracold polar molecules, Phys. Rev. Lett. **107**, 115301 (2011).
[11] A. V. Gorshkov, S. R. Manmana, G. Chen, E. Demler, M. D. Lukin, and A. M. Rey, Quantum magnetism with polar alkali-metal dimers, Phys. Rev. A **84**, 033619 (2011).
[12] M. A. Baranov, M. Dalmonte, G. Pupillo, and P. Zoller, Condensed matter theory of dipolar quantum gases, Chem. Rev. **112**, 5012 (2012).

[13] S. L. Cornish, M. R. Tarbutt, and K. R. A. Hazzard, Quantum computation and quantum simulation with ultracold molecules, Nat. Phys. **20**, 730 (2024).
[14] R. Zadoyan, D. Kohen, D. A. Lidar, and V. A. Apkarian, The manipulation of massive ro-vibronic superpositions using time–frequency-resolved coherent anti-Stokes Raman scattering (TFRCARS): From quantum control to quantum computing, Chem. Phys. **266**, 323 (2001).
[15] D. DeMille, Quantum computation with trapped polar molecules, Phys. Rev. Lett. **88**, 067901 (2002).
[16] A. André, D. DeMille, J. M. Doyle, M. D. Lukin, S. E. Maxwell, P. Rabl, R. J. Schoelkopf, and P. Zoller, A coherent all-electrical interface between polar molecules and mesoscopic superconducting resonators, Nat. Phys. **2**, 636 (2006).
[17] P. Rabl, D. DeMille, J. M. Doyle, M. D. Lukin, R. J. Schoelkopf, and P. Zoller, Hybrid quantum processors: Molecular ensembles as quantum memory for solid state circuits, Phys. Rev. Lett. **97**, 033003 (2006).
[18] S. Ospelkaus, K.-K. Ni, D. Wang, M. H. G. De Miranda, B. Neyenhuis, G. Quéméner, P. S. Julienne, J. L. Bohn, D. S. Jin, and J. Ye, Quantum-state controlled chemical reactions of ultracold potassium-rubidium molecules, Science **327**, 853 (2010).
[19] J. W. Park, S. A. Will, and M. W. Zwierlein, Ultracold dipolar gas of fermionic $^{23}Na^{40}K$ molecules in their absolute ground state, Phys. Rev. Lett. **114**, 205302 (2015).
[20] L. De Marco, G. Valtolina, K. Matsuda, W. G. Tobias, J. P. Covey, and J. Ye, A degenerate Fermi gas of polar molecules, Science **363**, 853 (2019).
[21] M.-G. Hu, Y. Liu, D. D. Grimes, Y.-W. Lin, A. H. Gheorghe, R. Vexiau, N. Bouloufa-Maafa, O. Dulieu, T. Rosenband, and K.-K. Ni, Direct observation of bimolecular reactions of ultracold KRb molecules, Science **366**, 1111 (2019).
[22] A. Schindewolf, R. Bause, X.-Y. Chen, M. Duda, T. Karman, I. Bloch, and X.-Y. Luo, Evaporation of microwave-shielded polar molecules to quantum degeneracy, Nature (London) **607**, 677 (2022).
[23] M. Duda, X.-Y. Chen, R. Bause, A. Schindewolf, I. Bloch, and X.-Y. Luo, Long-lived fermionic Feshbach molecules with tunable p-wave interactions, Phys. Rev. A **107**, 053322 (2023).
[24] P. K. Molony, P. D. Gregory, Z. Ji, B. Lu, M. P. Köppinger, C. R. Le Sueur, C. L. Blackley, J. M. Hutson, and S. L. Cornish, Creation of ultracold $^{87}Rb^{133}Cs$ molecules in the rovibrational ground state, Phys. Rev. Lett. **113**, 255301 (2014).
[25] T. Takekoshi, L. Reichsöllner, A. Schindewolf, J. M. Hutson, C. R. Le Sueur, O. Dulieu, F. Ferlaino, R. Grimm, and H.-C. Nägerl, Ultracold dense samples of dipolar RbCs molecules in the rovibrational and hyperfine ground state, Phys. Rev. Lett. **113**, 205301 (2014).
[26] X. Ye, M. Guo, M. L. González-Martínez, G. Quéméner, and D. Wang, Collisions of ultracold $^{23}Na^{87}Rb$ molecules with controlled chemical reactivities, Sci. Adv. **4**, eaaq0083 (2018).
[27] P. D. Gregory, M. D. Frye, J. A. Blackmore, E. M. Bridge, R. Sawant, J. M. Hutson, and S. L. Cornish, Sticky collisions of ultracold RbCs molecules, Nat. Commun. **10**, 3104 (2019).
[28] P. Gersema, K. K. Voges, M. Meyer zum Alten Borgloh, L. Koch, T. Hartmann, A. Zenesini, S. Ospelkaus, J. Lin, J. He, and D. Wang, Probing photoinduced two-body loss of ultracold nonreactive bosonic $^{23}Na^{87}Rb$ and $^{23}Na^{39}K$ molecules, Phys. Rev. Lett. **127**, 163401 (2021).
[29] N. Bigagli, W. Yuan, S. Zhang, B. Bulatovic, T. Karman, I. Stevenson, and S. Will, Observation of Bose–Einstein condensation of dipolar molecules, Nature (London) **631**, 289 (2024).
[30] K.-K. Ni, S. Ospelkaus, D. Wang, G. Quéméner, B. Neyenhuis, M. H. G. de Miranda, J. L. Bohn, J. Ye, and D. S. Jin, Dipolar collisions of polar molecules in the quantum regime, Nature (London) **464**, 1324 (2010).
[31] B. Zhu, G. Quéméner, A. M. Rey, and M. J. Holland, Evaporative cooling of reactive polar molecules confined in a two-dimensional geometry, Phys. Rev. A **88**, 063405 (2013).
[32] J. Söding, D. Guéry-Odelin, P. Desbiolles, G. Ferrari, and J. Dalibard, Giant spin relaxation of an ultracold cesium gas, Phys. Rev. Lett. **80**, 1869 (1998).
[33] T. Weber, J. Herbig, M. Mark, H.-C. Nägerl, and R. Grimm, Three-body recombination at large scattering lengths in an ultracold atomic gas, Phys. Rev. Lett. **91**, 123201 (2003).
[34] M. Guo, X. Ye, J. He, M. L. González-Martínez, R. Vexiau, G. Quéméner, and D. Wang, Dipolar collisions of ultracold ground-state bosonic molecules, Phys. Rev. X **8**, 041044 (2018).
[35] M. Horvath, S. Dhar, A. Das, M. D. Frye, Y. Guo, J. M. Hutson, M. Landini, and H.-C. Nägerl, Bose-Einstein condensation of non-ground-state caesium atoms, Nat. Commun. **15**, 3739 (2024).
[36] S. Peng, H. Liu, J. Li, and L. Luo, Collisional cooling of a Fermi gas with three-body recombination, Commun. Phys. **7**, 1 (2024).
[37] W. G. Tobias, K. Matsuda, G. Valtolina, L. De Marco, J.-R. Li, and J. Ye, Thermalization and sub-Poissonian density fluctuations in a degenerate molecular Fermi gas, Phys. Rev. Lett. **124**, 033401 (2020).
[38] E. Braaten and H. W. Hammer, Universal relation for the inelastic two-body loss rate, J. Phys. B **46**, 215203 (2013).
[39] M. He, C. Lv, H.-Q. Lin, and Q. Zhou, Universal relations for ultracold reactive molecules, Sci. Adv. **6**, eabd4699 (2020).
[40] L. Pan, X. Chen, Y. Chen, and H. Zhai, Non-Hermitian linear response theory, Nat. Phys. **16**, 767 (2020).
[41] X.-Y. Gao, D. Blume, and Y. Yan, Temperature-dependent contact of weakly interacting single-component Fermi gases and loss rate of degenerate polar molecules, Phys. Rev. Lett. **131**, 043401 (2023).
[42] X.-Y. Gao and Y. Yan, companion paper, Inelastic quantum Boltzmann equation of single-component Fermi gases, Phys. Rev. A, 043312 (2025).
[43] E. Braaten, H.-W. Hammer, and G. P. Lepage, Lindblad equation for the inelastic loss of ultracold atoms, Phys. Rev. A **95**, 012708 (2017).
[44] P. He, T. Bilitewski, C. H. Greene, and A. M. Rey, Exploring chemical reactions in a quantum degenerate gas of polar molecules via complex formation, Phys. Rev. A **102**, 063322 (2020).

[45] C. Wang, C. Liu, and Z.-Y. Shi, Complex contact interaction for systems with short-range two-body losses, Phys. Rev. Lett. **129**, 203401 (2022).
[46] D. Rossini, A. Ghermaoui, M. B. Aguilera, R. Vatré, R. Bouganne, J. Beugnon, F. Gerbier, and L. Mazza, Strong correlations in lossy one-dimensional quantum gases: From the quantum Zeno effect to the generalized Gibbs ensemble, Phys. Rev. A **103**, L060201 (2021).
[47] L. Rosso, A. Biella, and L. Mazza, The one-dimensional Bose gas with strong two-body losses: The effect of the harmonic confinement, SciPost Phys. **12**, 044 (2022).
[48] J. Maki, L. Rosso, L. Mazza, and A. Biella, Loss-induced collective mode in one-dimensional Bose gases, Phys. Rev. A **110**, 043315 (2024).
[49] N. P. Mehta, S. T. Rittenhouse, J. P. D'Incao, J. von Stecher, and C. H. Greene, General theoretical description of N-body recombination, Phys. Rev. Lett. **103**, 153201 (2009).
[50] L. De Marco, G. Valtolina, K. Matsuda, W. Tobias, J. Covey, and J. Ye, Replication data for: A degenerate Fermi gas of polar molecules (2019), 10.7910/DVN/RLOBHV.
[51] N. Navon, R. P. Smith, and Z. Hadzibabic, Quantum gases in optical boxes, Nat. Phys. **17**, 1334 (2021).
[52] F. Gerbino, I. Lesanovsky, and G. Perfetto, Large-scale universality in quantum reaction-diffusion from Keldysh field theory, Phys. Rev. B **109**, L220304 (2024).
[53] C. A. Regal, C. Ticknor, J. L. Bohn, and D. S. Jin, Tuning p-wave interactions in an ultracold Fermi gas of atoms, Phys. Rev. Lett. **90**, 053201 (2003).
[54] J. Zhang, E. G. M. van Kempen, T. Bourdel, L. Khaykovich, J. Cubizolles, F. Chevy, M. Teichmann, L. Tarruell, S. J. J. M. F. Kokkelmans, and C. Salomon, P-wave Feshbach resonances of ultracold ^{6}Li, Phys. Rev. A **70**, 030702(R) (2004).
[55] C. H. Schunck, M. W. Zwierlein, C. A. Stan, S. M. F. Raupach, W. Ketterle, A. Simoni, E. Tiesinga, C. J. Williams, and P. S. Julienne, Feshbach resonances in fermionic ^{6}Li, Phys. Rev. A **71**, 045601 (2005).
[56] K. Günter, T. Stöferle, H. Moritz, M. Köhl, and T. Esslinger, p-wave interactions in low-dimensional fermionic gases, Phys. Rev. Lett. **95**, 230401 (2005).
[57] Y. Inada, M. Horikoshi, S. Nakajima, M. Kuwata-Gonokami, M. Ueda, and T. Mukaiyama, Collisional properties of p-wave Feshbach molecules, Phys. Rev. Lett. **101**, 100401 (2008).
[58] J. Fuchs, C. Ticknor, P. Dyke, G. Veeravalli, E. Kuhnle, W. Rowlands, P. Hannaford, and C. J. Vale, Binding energies of ^{6}Li p-wave Feshbach molecules, Phys. Rev. A **77**, 053616 (2008).
[59] R. A. W. Maier, C. Marzok, C. Zimmermann, and Ph. W. Courteille, Radio-frequency spectroscopy of ^{6}Li p-wave molecules: Towards photoemission spectroscopy of a p-wave superfluid, Phys. Rev. A **81**, 064701 (2010).
[60] M. Gerken, B. Tran, S. Häfner, E. Tiemann, B. Zhu, and M. Weidemüller, Observation of dipolar splittings in high-resolution atom-loss spectroscopy of ^{6}Li p-wave Feshbach resonances, Phys. Rev. A **100**, 050701(R) (2019).
[61] Y. Kiefer, M. Hachmann, and A. Hemmerich, Ultracold Feshbach molecules in an orbital optical lattice, Nat. Phys. **19**, 794 (2023).
[62] V. Venu, P. Xu, M. Mamaev, F. Corapi, T. Bilitewski, J. P. D'Incao, C. J. Fujiwara, A. M. Rey, and J. H. Thywissen, Unitary p-wave interactions between fermions in an optical lattice, Nature (London) **613**, 262 (2023).
[63] R. R. W. Wang, S. Biswas, S. Eppelt, F. Deng, X.-Y. Luo, and J. L. Bohn, Simulations of evaporation to deep Fermi degeneracy in microwave-shielded molecules, Phys. Rev. A **110**, 043309 (2024).